



# Genome-Wide Association Studies of Salt Tolerance at Seed Germination and Seedling Stages in *Brassica napus*

Guofang Zhang<sup>1,2</sup>, Jinzhi Zhou<sup>1</sup>, Yan Peng<sup>1</sup>, Zengdong Tan<sup>1,2</sup>, Long Li<sup>1,2</sup>, Liangqian Yu<sup>1,2</sup>, Cheng Jin<sup>1</sup>, Shuai Fang<sup>1,2</sup>, Shaoping Lu<sup>1,2</sup>, Liang Guo<sup>1,2</sup> and Xuan Yao<sup>1,2\*</sup>

<sup>1</sup> National Key Laboratory of Crop Genetic Improvement, Huazhong Agricultural University, Wuhan, China, <sup>2</sup> Hubei Hongshan Laboratory, Wuhan, China

## OPEN ACCESS

### Edited by:

Zhi Qi,  
Inner Mongolia University, China

### Reviewed by:

Ricardo Mir,  
Universitat Politècnica de València,  
Spain  
Kun Lu,  
Southwest University, China

### \*Correspondence:

Xuan Yao  
xuanyao@mail.hzau.edu.cn

### Specialty section:

This article was submitted to  
Plant Abiotic Stress,  
a section of the journal  
Frontiers in Plant Science

**Received:** 08 September 2021

**Accepted:** 25 November 2021

**Published:** 05 January 2022

### Citation:

Zhang G, Zhou J, Peng Y, Tan Z, Li L, Yu L, Jin C, Fang S, Lu S, Guo L and Yao X (2022) Genome-Wide Association Studies of Salt Tolerance at Seed Germination and Seedling Stages in *Brassica napus*. *Front. Plant Sci.* 12:772708. doi: 10.3389/fpls.2021.772708

Most crops are sensitive to salt stress, but their degree of susceptibility varies among species and cultivars. In order to understand the salt stress adaptability of *Brassica napus* to salt stress, we collected the phenotypic data of 505 *B. napus* accessions at the germination stage under 150 or 215 mM sodium chloride (NaCl) and at the seedling stage under 215 mM NaCl. Genome-wide association studies (GWAS) of 16 salt tolerance coefficients (STCs) were applied to investigate the genetic basis of salt stress tolerance of *B. napus*. In this study, we mapped 31 salts stress-related QTLs and identified 177 and 228 candidate genes related to salt stress tolerance were detected at germination and seedling stages, respectively. Overexpression of two candidate genes, *BnCKX5* and *BnERF3* overexpression, were found to increase the sensitivity to salt and mannitol stresses at the germination stage. This study demonstrated that it is a feasible method to dissect the genetic basis of salt stress tolerance at germination and seedling stages in *B. napus* by GWAS, which provides valuable loci for improving the salt stress tolerance of *B. napus*. Moreover, these candidate genes are rich genetic resources for the following exploration of molecular mechanisms in adaptation to salt stress in *B. napus*.

**Keywords:** salt stress, germination stage, seedling stage, GWAS, *Brassica napus*

## INTRODUCTION

Salt stress is a leading cause of inhibition of crop growth and development in the world (Munns, 2005; Morton et al., 2019). At present, about 10% area of China is arable land is salt-affected (Song and Liu, 2017). Although many methods have been used to improve the high yield of crops under salt stress, it is also a challenge of maintaining the world food supplies (Hickey et al., 2019; Tyerman and Munns, 2019). Understanding the genetic and molecular mechanisms for enhancing salt tolerance is an important step toward improving the agricultural productivity of crops (Patishtan et al., 2018).

Salt stress mainly includes ion stress and osmotic stress (Zhu, 2002; Julkowska and Testerink, 2015). Short-term salt stress can make the plants immediately appear the phenomenon of wilting

dehydration and slow down the growth speed of the new leaves slow down. However, long-term salt stress can cause ion poisoning and a high concentration of ions in the old leaves, leading to falling off of leaves. Crops have different abilities to resist salt stress. When the level of salt stress is greater than the resistance of plants, owing to cell membrane damage, ion imbalance, lipid peroxidation, reactive oxygen species production and metabolic disorders, etc., the damage of high osmotic pressure will restrict the normal growth and development of plants (Bedard and Krause, 2007; Munns and Tester, 2008). Moreover, Salt stress is mainly regulated by hormones and ion transporters in plants, which form a complex genetic regulatory network (Zhu, 2001b, 2016; Khan and Hakeem, 2013).

The harm of salt stress is also attributed to inhibition of moisture absorption and ions poisoning and their interference with the uptake of mineral nutrients based on a decrease in osmotic potential (Khan and Weber, 2006; Mba et al., 2007). HKT1 encodes a sodium ion ( $\text{Na}^+$ ) transporter and it contributes to salt tolerance in plants (Apse et al., 1999; Brini et al., 2007). The SOS signaling pathway was involved in  $\text{Na}^+$  extrusion (Ma et al., 2019). The *sos* mutants show hypersensitivity to salt stress in *Arabidopsis* (Zhu, 2001a; Shi et al., 2002), whereas overexpression of *AtSOS1*, *AtSOS2*, and *AtSOS3*-overexpression can significantly improve salt resistance in plants (Zhu, 2001a, 2016). *OsSKC1* was mapped for root and shoot  $\text{Na}^+$ /potassium ion ( $\text{K}^+$ ) concentration and transportation in the shoots and roots controlling rice salt tolerance (Lin et al., 2004). Two  $\text{Na}^+/\text{H}^+$  antiporters, *AtNHX1* and *AtNHX2*, localized on the tonoplast membrane. They are expressed in roots and leaves, and selectively transports  $\text{Na}^+$  into the vacuole. *nhx1* and *nhx2* mutants showed decreased sensitivity to salt stress in *Arabidopsis* (Brini et al., 2007; Barragan Borrero et al., 2012).

Salt stress usually makes a significant inhibitory effect on seed germination and seedling growth of crops, which plays an important role in stable stand establishment and yield of crops (Rehman et al., 2000). Previous studies have shown that germination rate, shoot length, root length, and aboveground dry weight at the seed germination stage are extremely sensitive to salt stress in crops (Gomes-Filho et al., 2008; Munns et al., 2012; Yu et al., 2018). Moreover, plant height, root length,  $\text{Na}^+/\text{K}^+$  ratio, relative electrical conductivity, aboveground fresh weight, and dry weight can also be affected by salt stress during the seedling period in rice (Campbell et al., 2015), wheat, barley (Fan et al., 2016), tomato (Campbell et al., 2015), *Arabidopsis* (Awlia et al., 2016), and *B. napus* (Hou et al., 2017; Lang et al., 2017). To date, only a few studies have focused on the gene function related to salt stress tolerance of *B. napus*. The *AtNHX1* overexpression could significantly improve the salt tolerance of *B. napus* (Zhang et al., 2001). The *BnaABF2* could significantly enhance salt tolerance in transgenic *Arabidopsis* (Zhao et al., 2016). The 582 transcription factors and 438 transporter genes have been identified by a comparative transcriptome analysis under salt stress (Yong et al., 2014). With the development of sequencing technology, genome-wide association study (GWAS) is a quick tool to map QTLs of complex traits for crop genetic improvement (Pearson and Manolio, 2008; De et al., 2014). *Bna.SCO1*, *Bna.ARR4*, and *Bna.ATE1* was identified at the germination stage under salt stress

by GWAS in 248 *B. napus* accessions using the 60k SNP array (Hatzig et al., 2015). In addition, 38 promising candidate genes associated with salt tolerance were also identified by GWAS in 368 Brassica accessions using a 60k SNP array (Wan et al., 2017). A total of 62 QTLs for aboveground dry weight and  $\text{Na}^+/\text{K}^+$  ratio traits were identified in 85 *B. napus* inbred lines (Yong et al., 2015). GWAS could improve efficiency and cost savings to parse the genetic basis based on abundant genetic variation and prediction precision (Huang et al., 2012). *OsMADS31* could be a down-regulated expression and was identified by GWAS to be a candidate gene related to salt stress response at the germination stage of rice (Yu et al., 2018). Although a great number of QTLs and candidate genes have been identified by previous studies in *B. napus*, no candidate genes are functionally validated in response to salt stress and molecular mechanisms underlying the regulation of salt tolerance have not been elucidated in *B. napus*.

To study the genetic basis of the adaptation of *B. napus* to salt stress, GWAS of salinity-stress responsive traits at seed germination and seedling stages in the 505 *B. napus* accessions was employed to map QTLs related to the salt stress responses. Here we totally identified 177 and 228 candidate genes controlling 16 salt stress coefficients (STCs) of *B. napus* subjected to salt stress at seed germination and seedling stages, respectively. It should be noted that many previously unreported genes were discovered to be involved in salt stress responses. This study will help us unveil the mechanism of salt stress adaptation and provide a valuable reference for the genetic improvement of salt tolerance in *B. napus*.

## MATERIALS AND METHODS

### Materials

A collection consisting of 505 natural accessions of *B. napus* (Supplementary Table 1; Tang et al., 2021) was used to investigate growth in normal and salt stress conditions at seed germination and seedling stages (Supplementary Table 2).

### Trait Measurement at Seed Germination and Seedling Stages

The experiment involved 100 uniform seeds which were treated by three treatment groups including normal (CK), low salt (150 mM sodium chloride [ $\text{NaCl}$ ]), and high salt stress (215 mM  $\text{NaCl}$ ) and put into a Petri dish ( $\Phi$  9 cm, Guangzhou Jietae Biological Filtration Co., Ltd., Wuhan, China) with double layers of filter paper ( $\Phi$  9 cm, General Electric Biotech Hangzhou Co., Ltd., Wuhan, China). Then, we added 10 ml deionized water (CK), 150 mM (T1), and 215 mM (T2)  $\text{NaCl}$  solution into the petri dish with a petri dish cover in the growth room for 3 days, 7 days, and 2 weeks to record germination potential (FYS), germination rate (FYL), shoot length (SL), and root length (RL), respectively (Supplementary Figure 1). All experiments were carried out in a greenhouse with 25/16°C day/night temperature under a 16/8 h of light/darkness photoperiod and 50–60% RH (Long et al., 2015).

For measurements at the seedling stage, the plants were grown in ten rounds of experiments, and each round contained about

50 accessions. We designed 2 treatment groups including normal (CK) and high salt stress (215 mM NaCl solution) conditions with 6 biological repeats per line (**Supplementary Figure 2**). In order to guarantee reliability, we firstly selected 25–30 uniform and healthy seeds and then put the seeds into the yarn net in hydroponic culture for a generation. After 10 days, the uniform seedlings were selected and transferred to a 10 L black box covered by a black plate with Hoagland nutrient solution (60 cm length × 40 cm width × 10 cm depth) according to a completely randomized block design. After these plants were cultivated in the nutrient solution culture for about 2 weeks, we added 10 L Hoagland nutrient solution (CK) and Hoagland nutrient solution containing 215 mM (T2) NaCl solution into the black box, respectively, and the nutrient solution was changed once a week. The seedlings were treated for 2 weeks in the hydroponic culture. Hoagland nutrient solution consists of the following nutrients: 4 mM KNO<sub>3</sub>, 1 mM MgSO<sub>4</sub>, 4 mM Ca (NO<sub>3</sub>)<sub>2</sub>, 1 mM NH<sub>4</sub>H<sub>2</sub>PO<sub>4</sub>, 1 mM (NH<sub>4</sub>)<sub>2</sub>HPO<sub>4</sub>, 1 mM NaCl, 41.2 μM Na<sub>2</sub>-EDTA, 12.5 μM H<sub>3</sub>BO<sub>3</sub>, 0.39 μM CuSO<sub>4</sub>, 1.59 μM MnSO<sub>4</sub>, 1 μM ZnCl<sub>2</sub>, and 0.5 μM NaMoO<sub>4</sub>, and pH of the solution was adjusted to 5.8 with 0.1 M KOH (Sinopharm Chemical Reagent Co., Ltd., Wuhan, China) (Monirifar and Barghi, 2009; Wan et al., 2017).

## Determination of Growth Indexes

### Growth Indexes

After a 2-week salt treatment, some traits, such as plant height (PH), RL, aboveground dry weight (ADW), and root dry weight (RDW) were measured. Materials were harvested and dried at 85°C for at least 72 h to be weighed (Lv et al., 2016; Yu et al., 2017).

### Leaf Area

Leaf area was measured by a high-throughput leaf area meter developed by the phenotyping platform of phenotype platform center of Huazhong Agricultural University (Yang et al., 2015).

### Leaf Chlorophyll Content

Leaf chlorophyll content was determined using the Chlorophyll Meter SPAD-502plus (Spectrum Technologies Inc., Hangzhou, China) under salt stress and normal conditions. The fully-expanded penultimate leaf was used for the measurement. Each leaf was measured three times at different positions avoiding the veins, and the average of the three readings was recorded at different time points under salt stress conditions (Kang et al., 2019).

### Determination of Proline

Proline was an important component of plants in response to salt stress. L-proline concentration was determined using a standard curve. About 0.1 g of leaves were homogenized in 1.5 ml of 3% sulfosalicylic acid (Sinopharm Chemical Reagent Co., Ltd., Wuhan, China) and the residue was removed by centrifugation at 3,000 rpm/min for 5 min. 100 μl of the extract was reacted with 2 ml glacial acetic acid and 2 ml acid ninhydrin (Sinopharm Chemical Reagent Co., Ltd., Wuhan, China) (1.25 g acid ninhydrin warmed in 30 ml glacial acetic acid and 20 ml 6 M phosphoric acid until dissolved) for 1 h at 100°C and

the reaction was then terminated in an ice bath. The reaction mixture was extracted with 1 ml toluene. The vortex shocked for 30 s and rested 10 min. The chromophore-containing toluene was warmed to room temperature and its optical density was measured at 520 nm *via* an ultra-microporous plate (MPP) spectrophotometer (BioTek Epoch, United States) (Bates et al., 1973; Khedr et al., 2015).

### Determination of Malondialdehyde

We weighed approximately 0.1 g of leaf tissue per plant, to which we added 2 ml of 10% trichloroacetic acid (TCA, Sinopharm Chemical Reagent Co., Ltd., Wuhan, China) solution followed by the addition of to achieve a total volume of 3 ml. The samples have subsequently centrifuged the sample for 10 min, at 4°C at 4,000 rpm. We transferred 2 ml solution of the supernatant into new tubes and added 2 ml of distilled water and 2 ml of 0.6% thiobarbituric acid (TBA, Sinopharm Chemical Reagent Co., Ltd., Wuhan, China) solution, respectively. After a 15-min reaction in boiling water for a 15 min reaction, after which the solution was centrifuged and cooled to room temperature. Finally, we measured the malondialdehyde (MDA) content at wavelengths of 450, 532, and 600 nm *via* an ultra-microporous plate (MPP) spectrophotometer (BioTek Epoch, United States) (Hong et al., 2005; Wang et al., 2006).

### Relative Electrical Conductivity

Relative electrical conductivity measurements were performed as previously described with minor modifications (Lv et al., 2016). One fully expanded functional leaf from normal plants was cut into segments of similar sizes by a leaf blade sampler and immersed in 8 ml of double-distilled water in a 10 ml tube for 24 h at room temperature with continual shaking at 100 rpm, and then we calculated the parameter (S1) by a conductivity meter (Model DDS-IIA, Shanghai Leici Instrument, Inc., Shanghai, China). The rest of the solution was placed into a water bath at 100°C for 10 min. After the sample was cooled down to room temperature, the conductivity value was measured (S2) (Model DDS-IIA, Shanghai Leici Instrument, Inc., Shanghai, China). The value of REC was calculated as the ratio of S1 to S2.

### Statistical Analysis

Student's *t*-test was performed to calculate the statistically significant differences between data sets. For each accession, the absolute values of all traits were obtained and the average of 6 replicates was counted under each condition. The salt tolerance coefficient was calculated by  $STC = T/WT$ . We used the scale package of R language to analyze data standardization. Phenotypic data were analyzed using the stat.desc package of R language.

### Genetic, Treatment Effect, and Heritability Analysis

To determine the variance components, we used mixed-effect ANOVA of avo package of R language including the genetic effect (G\_effect), treatment effect (E\_effect), and interaction effect of genetic and treatment effect (G & E effect). Broad sense heritability ( $H_2b$ ) was calculated for all traits as follows:  $H_2b = \sigma^2_G / (\sigma^2_G + \sigma^2_{GE}/n + \sigma^2_e/nr)$  where  $\sigma^2_G$  was the genotypic variance,  $\sigma^2_e$  was the error variance,  $\sigma^2_{GE}$  is the variance of

the genotype by environment interaction and  $r$  is the number of replications with R language. The estimates of  $\sigma^2_G$  and  $\sigma^2_e$  were analyzed by the ANOVA using the lmer function in the lme4 package in the R environment. All statistical analyses were performed in R language (Chen et al., 2014).

### Correlation Analysis

The correlation coefficient was calculated using the corr.test of psych package and plotted using the corrplot package of R language.

### Genome-Wide Association Analysis

The 505 *B. napus* accessions were collected to construct this association panel (Tang et al., 2021). The high-quality clean reads data was used by the BWA (version 0.75) software (Li and Durbin, 2009). The reference genome came from “Brassica version 4.1” (‘Darmor-bzh’ genome<sup>1</sup>). We adopted a mixed-model approach using the factorial spectrally transformed linear mixed model with 6,448,413 SNPs (MAF > 0.05). We also performed GWAS using FaST-LMM software models (Listgarten et al., 2013).

### Identification of Candidate Genes and Polymorphisms

The suggestive and significant  $P$ -value thresholds of the entire population were  $1.0e-06$ . All SNPs that exceeded the significance criterion were assessed for the location of candidate genes. If coding regions were present, the potential impact on the protein of each SNP was subsequently determined using the “Allele finder” facility Gene Ontology (GO) analysis. The candidate genes with differential gene expression ratios between the control treatment and stress treatment ( $R \geq 2$  or  $\leq 0.5$ ) (Zhang et al., 2019) were identified within 200 kb upstream or downstream of the lead SNP (Tang et al., 2021).

### RNA-Seq

Total RNA was extracted with TRIzol reagent (Invitrogen Life Technologies, Wuhan, China) from the leaves of 4-week-old plants grown under normal conditions and 385 mM NaCl in a growth chamber set at 25°C, a 16/8 h light/dark and 50–60% relative humidity. The RNA was dissolved in DEPC water and measured with a spectrophotometer (NanoDrop, Beijing, China, 2000). The purified RNA was sequenced with GenoSeq (high-throughput phenotyping://www.genoseq.cn/) using an Illumina HiSeq platform center of Huazhong Agricultural University in paired-end  $2 \times 150$  bp mode, and approximately 10 Gb of clean reads were generated for each sample. We finally calculated the normalized transcripts per million (TPM) values. (Supplementary Table 15).

### Generation of Overexpression Transgenic Plants

The coding DNA sequences of BnaA02g05340D (*BnCKX5*, Primer\_F: CGGGGTACCGCCACCATGATAGCTTACATAGAGCCATACT, Primer\_R: GCTCTAGATCATTTGTCGTCGTCGTCCTTGTAGTCCATAGGAGCCCTATTGAAAATCTTTTG) and BnaA06g02670D (*BnERF3*, Primer\_F: CGGGGTACC

GCCACCATGAGGAGAGGTAGAGTCTCT, Primer\_R: GCTCTAGATTATTTGTCGTCGTCGTCCTTGTAGTCCATGAGAGGTAGATCGGTGCATAT, Tsingke Biological Technology Wuhan Co., Ltd., Wuhan, China) were cloned from accession X182 (97097), and the cloned fragments were subsequently ligated into pCAMBIA-1300s using the *KpnI* and *XbaI* restriction enzymes. Cloning primers and sequencing primers are from Tsingke Biological Technology Wuhan Co., Ltd Wuhan, China. The accession, specifically Westar, was used as the transgenic receptor material. *Agrobacterium tumefaciens*-mediated transformation was performed in *B. napus* as previously described (Dai et al., 2020).

### Salt and Mannitol Treatments on Overexpression Transgenic Plants

A total of 50 seeds of *OE-BnCKX5*, *OE-BnERF3*, and Westar (WT) were sown into Petri dishes with covers on them and grown in a greenhouse at 25/16°C day/night temperature under a 16/8 h light/dark photoperiod and 50–60% RH. *OE-BnCKX5* lines and WT were treated by 0, 50, 100, 125, 150, and 200 mM NaCl and mannitol for 9 days, respectively. *OE-BnERF3* lines and WT were treated by 0, 50, 100, 125, 150, 175, 200, and 225 mM NaCl and mannitol for 9 days, respectively. Germination rate, stem length, and root length were determined after the salt and mannitol treatments.

## RESULTS

### Phenotypic Variation in 505 *Brassica napus* Accessions for Salt Tolerance Traits at Germination and Seedling Stages

To study the response of the 505 *B. napus* accessions to salt stress, we analyzed the related traits at the germination stage under 0 mM, 150 mM (T1), and 215 mM NaCl (T2), and at the seedling stage under 0 mM and 215 mM NaCl (T2). The germination potential (FYS\_CK, FYS\_T1, and FYS\_T2), germination rate (FYL\_CK, FYL\_T1, and FYL\_T2), shoot length (GSL\_CK and GSL\_T1), and root length (GRL\_CK and GRL\_T1) at the germination stage were measured (Supplementary Tables 2, 3). At the seedling stage, we obtained traits under the normal and salt stress conditions, such as plant height (PH\_CK and PH\_T2), root length (RL\_CK and RL\_T2), root dry weight (RDW\_CK and RDW\_T2), aboveground dry weight (ADW\_CK and ADW\_T2), total dry weight (TDW\_CK and TDW\_T2), leaf area (LA\_CK and LA\_T2), malondialdehyde content (MDA\_CK and MDA\_T2), proline content (Proline\_CK and Proline\_T2), chlorophyll content under (SPAD\_CK and SPAD\_T2), and relative electrical conductivity (REC\_CK and REC\_T2) (Supplementary Tables 2, 4). In order to better reflect salt stress responses, we focused on the salt tolerance coefficient (STC) calculated as the ratio of trait value under salt stress condition to that under normal condition, which was represented by the suffix type “trait\_R1” under low salt stress and “trait\_R2” under high salt stress (Supplementary Table 5; Guo et al., 2018). Descriptive statistics

<sup>1</sup><https://www.genoscope.cns.fr/brassicnapus/data/>

is a good description of phenotypic variation in 505 *B. napus* accessions under normal and salt stress conditions. We calculated the descriptive statistics through “Mean,” “Max,” “Min,” “SD,” “SE,” and “CV” for the mean values (**Supplementary Table 6**). We found that most characters were, on average, reduced by more than 25% (CV,%) under salt stress (**Supplementary Table 6**). Most traits of the accessions show significant variations under salt stress conditions. Interestingly, large variations in germination potential (FYS) and germination rate (FYL) were observed among the accessions under salt stress, whereas FYS and FYL showed small variations under the normal conditions at the germination stage (**Supplementary Table 6**).

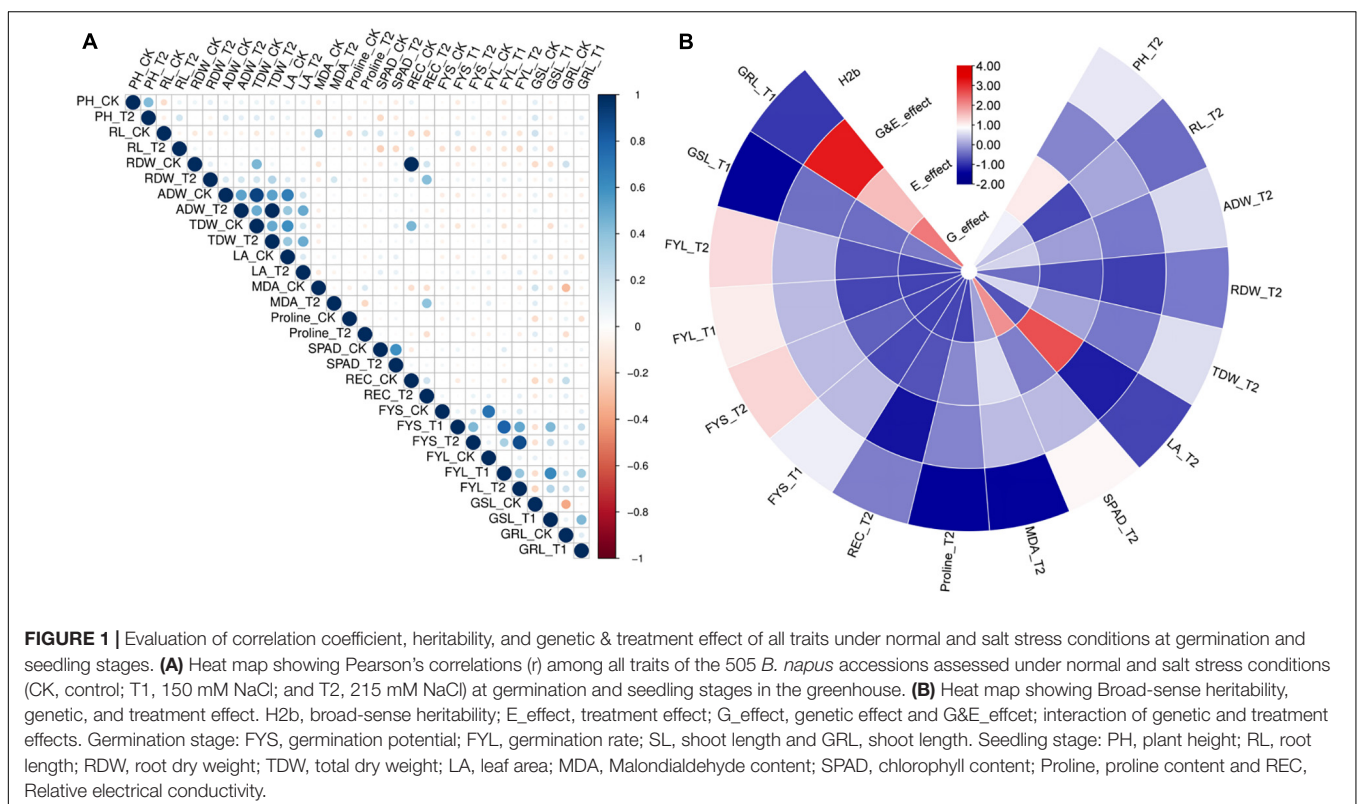
## Frequency Distribution and Correlation Analysis Among All Traits Under Salt Stress

We also performed normal distribution detection on the original value (**Supplementary Table 7**) and the relative value (STCs) for GWAS (**Supplementary Table 8**), respectively. Except for germination potential (FYS) and germination rate (FYL), the rest of the traits were found in normal and lognormal distributions. The non-normal distribution for FYS and FYL may be attributed to the significant phenotypic differences among these accessions. Correlation analysis for all traits at germination and seedling stages was calculated and presented in **Supplementary Table 9**. A total of 10 traits at the seedling stage and 4 traits at the germination stage showed significant correlations with  $r$ , which ranged from 0.001 to 0.994 between each other (**Figure 1A**,

**Supplementary Table 9**, and **Supplementary Figures 3–5**). It is worth noting that the RDW\_CK was strongly correlated with the TDW\_CK and REC\_CK ( $r \geq 0.4$ ). The RL\_CK was strongly correlated with the MDA\_CK ( $r \geq 0.3$ ). The RDW\_T2 was strongly correlated with the REC\_T2 and TDW\_T2 ( $r \geq 0.3$ ). The ADW\_T2 was strongly correlated with the ADW\_CK, TDW\_CK, TDW\_T2, LA\_CK, and LA\_T2 ( $r \geq 0.3$ ). The TDW\_CK was strongly correlated with the TDW\_T2, LA\_CK, and REC\_CK ( $r \geq 0.4$ ). Moreover, a strong positive correlation between normal and salt stress conditions was observed for PH, GDW, TDW, and SPAD, and their correlations were from 0.426 to 0.599. By comparing the growth dynamics of normal and salt-treated plants, the positive correlations were in accordance with observation between the traits related to salt stress.

## Heritability, Genetic, and Treatment Effect Analysis

Heritability is a key factor for marking decisions in crop breeding and it is crucial to make an effective design for the breeding scheme (Chen et al., 2014). We also calculated the broad heritability ( $H_2b$ ), which was presented in **Supplementary Table 10**. As for these parameters, variation between accessions was determined for a large part by the genotype, corresponding to low to high heritabilities ( $0.002 < H_2b < 0.66$ ) (**Figure 1B** and **Supplementary Table 10**). We found that the  $H_2b$  of these traits was more than 0.5 including plant height (PH), ground dry weight (ADB), total dry weight (TDW), and chlorophyll content (SPAD). Compared with the control, we always chose



significantly genetic and treatment effects of these traits under the different salt treatments using the AVOVA in the R environment ( $P \leq 0.05$ ). In addition, the genetic effect and treatment effect ( $G_{\text{effect}}$  and  $E_{\text{effect}}$ ,  $P \leq 0.05$ ) could significantly represent the genotype effect and environment effect, which were significant for all traits (Figure 1B and Supplementary Table 10). These results showed that normal growth and growth response to salt stress are dynamic traits that are determined for a large part by the genetic effect.

## Genome-Wide Association Studies Revealed QTLs Which Were Associated With Salt Stress in *Brassica napus* and Prediction of Candidate Genes Related to Salt Stress

Salt tolerance coefficient (STC) was usually described as an effective salt stress indicator. 16 STCs were performed using the Fast-LMM for GWAS (Listgarten et al., 2013; Figures 2A,B and Supplementary Table 5). The results showed that 5,410 ( $\sim 0.08\%$  of in total) strongly associated SNPs [ $-\log(P) \geq 6$ ] (Supplementary Table 11) were chosen to further map the QTLs with the largest effects. There were some co-localized SNPs

between leaf area (LA\_R2), chlorophyll content (SPAD\_R2), relative electrical conductivity (REC\_R2), and malondialdehyde (MDA\_R2) distributed on Chromosome A02 and A03. In addition, some SNPs were co-localized between chlorophyll content (SPAD\_R2) and root length (RL\_R2), leaf area (LA\_R2), and relative electrical conductivity (REC\_R2) distributed on Chromosome A02, A05, A06, and A10 at the seedling stage (Figure 2A and Supplementary Table 12). Some co-localized SNPs between FYL\_R2 and FYS\_R2 were also found to locate on Chromosome A07 and C01 at the germination stage (Supplementary Table 12 and Figure 2B). Some of these significant SNPs were in linkage disequilibrium and therefore considered to associate with the same causal genes or were assigned to the same QTL.

The candidate genes were selected within 200 kb upstream or downstream of a significant SNP (Supplementary Tables 13, 14). By differential expression analysis comparing normal and treatment conditions (the ratio  $\geq 2$  or  $\leq 0.5$ ) (Zhang et al., 2019), we finally identified 177 candidate genes at the germination stage (Supplementary Table 13) and 228 candidate genes (Supplementary Table 14) at the seedling stage, respectively. Based on our RNA-seq analysis, we also found that these candidate genes were significantly induced by salt stress.

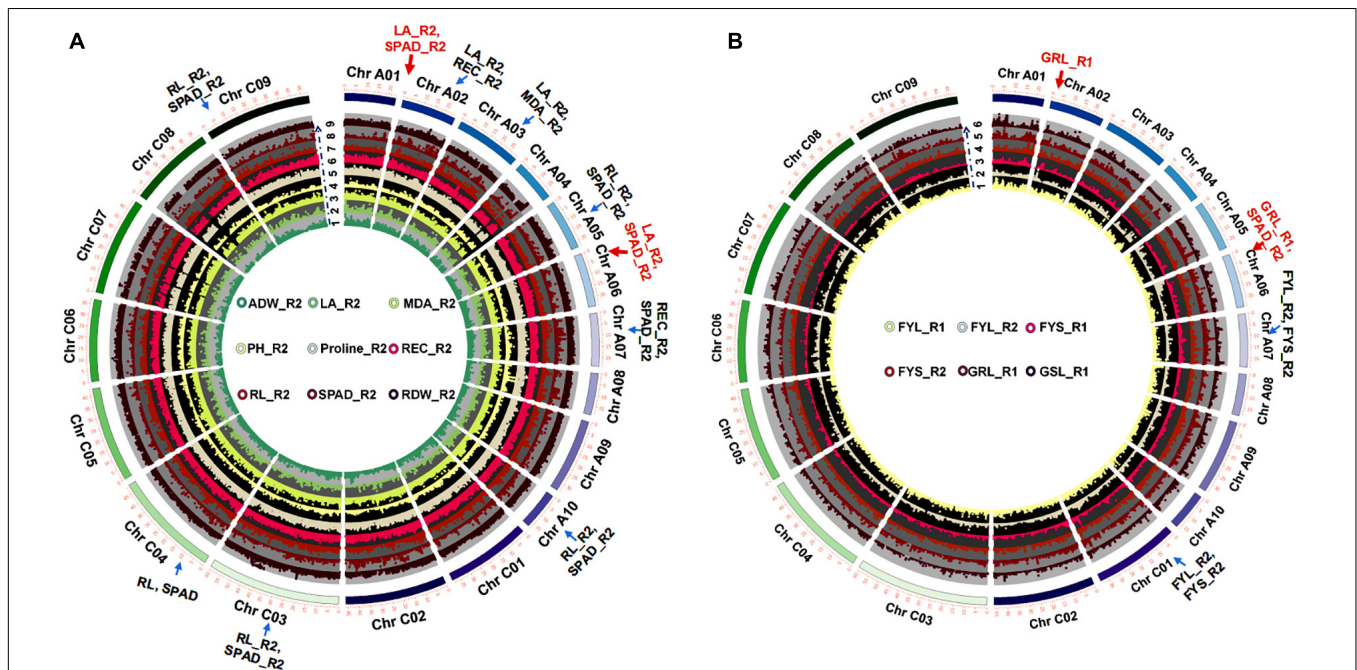


**FIGURE 2 |** GWAS of STCs at germination and seedling stages. **(A)** Circle Manhattan plots with the co-localized SNPs of multiple traits at the seedling stage ( $P$ -value  $\leq 1e-2$ ; arrows represent sites of co-located SNPs). 1: ADW\_R2, the ratio of aboveground dry weight between normal condition and 215 mM NaCl; 2: LA\_R2, the ratio of leaf area between normal condition and 215 mM NaCl; 3: MDA\_R2, the ratio of MDA content between normal condition and 215 mM NaCl; 4: PH\_R2, the ratio of plant height between normal condition and 215 mM NaCl; 5: Proline\_R2, the ratio of proline content between normal condition and 215 mM NaCl; 6: REC\_R2, the ratio of relative electrolyte leakage between normal condition and 215 mM NaCl; 7: RL\_R2, the ratio of root length between normal condition and 215 mM NaCl; 8: SPAD\_R2, the ratio of chlorophyll content between normal condition and 215 mM NaCl; 9: RDW\_R2, the ratio of root dry weight between normal condition and 215 mM NaCl. **(B)** Circle Manhattan plots with the co-localized SNPs of multiple traits at the germination stage ( $P$ -value  $\leq 1e-2$ ; arrows represent sites of co-located SNPs). 1: FYL\_R1, the ratio of germination rate between normal condition and 150 mM NaCl; 2: FYL\_R2, the ratio of germination rate between normal condition and 215 mM NaCl; 3: FYS\_R1, the ratio of germination potential between normal condition and 150 mM NaCl; 4: FYS\_R2, the ratio of germination potential between normal condition and 215 mM NaCl; 5: SL\_R1, the ratio of shoot length between normal condition and 150 mM NaCl; and 6: RL\_T1, the ratio of root length between normal condition and 150 mM NaCl.

Transcription levels of some candidate genes assayed by RNA-seq were shown as an example (Supplementary Tables 14, 15 and Supplementary Figure 6), which was consistent with the previous transcriptome analysis<sup>2</sup> (Zhang et al., 2019). Most of the candidate genes were found to be related to cellular processes, metabolic processes, biological regulation, signaling, and response to stimulus (Supplementary Figure 7). These results emphasized that complex genetic mechanisms of salt stress responses are regulated by multiple genes in both normal and salt stress conditions at germination and seedling stages.

### ***BnCKX5* Overexpression Increased the Sensitivity to Salt and Mannitol Stresses at the Germination Stage**

There are 36 genes on ChrA02 within 200 kb upstream and downstream of the candidate SNPs, BnvaA0202514802 and BnvaA0202514804 of LA\_R2, BnvaA0202449329 of SPAD\_R2 and BnvaA0201847086 of RL\_R1 (Figures 3A,B and Supplementary Table 14). Moreover, among these genes, BnaA02g05340D, whose expression was found to be significantly induced by salt stress and ABA treatment (Figure 3C, Supplementary Figures 6, 15, and Supplementary Table 17) (see text footnote 1) (Zhang et al., 2019), have not yet been reported to be related to salt stress in *B. napus*. Thus, we focused on the BnaA02g05340D for further study. BnaA02g05340D named *BnCKX5* is a homolog of *Arabidopsis* CKX5 belonging to CKXs subfamily VII, which encodes a cytokinin dehydrogenase and plays a vital role in maintaining cytokinin homeostasis (Ma et al., 2016). However, whether CKX5 plays a role in plant salt tolerance remains unknown (Liu et al., 2018). *BnCKX5* consists of three introns and four exons with pairwise LD correlations, which presents rich SNP sequence variations leading to amino acids changes ( $r^2 > 0.5$ ) (Figure 3D and Supplementary Table 18). The haplotypes of *BnCKX5* were grouped into 3 haplotypes including hap.A, hap.B, and hap.C types. The absolute and relative values of leaf area (LA) in the Hap.C type accessions were significantly less than that in hap.A and hap.B under salt stress (Figures 3E–G and Supplementary Table 19), while the absolute and relative values of chlorophyll content (SPAD) in the hap.C type accessions were significantly higher than that in hap.A and hap.B type accessions under normal and salt stress conditions (Figures 3H–J and Supplementary Table 19). Therefore, *BnCKX5* was considered as a candidate gene for salt stress response and showed a rich SNPs variation among 505 *B. napus* accessions. The identified extreme haplotypes related to salt tolerance would be useful for breeding salt-tolerant *B. napus* in the future.

To validate whether *BnCKX5* was involved in response to salt stress, seeds of *BnCKX5*-overexpressing (*OE-BnCKX5*) plants and WT were sowed under the 0, 50, 100, 125, 150, and 200 mmol NaCl for 9 days (Figure 3K and Supplementary Figures 8, 9). Germination rates significantly decreased in the *OE-BnCKX5* lines compared with the WT plants under the salt treatments (Figure 3L). Stem length and root lengths of

*OE-BnCKX5* lines were significantly lower than that of WT under 50 mmol NaCl (Figures 3M–O). In addition, seeds of *OE-BnCKX5* and WT have also sowed under 0, 50, 100, 125, 150, and 200 mmol mannitol for 9 days. Germination rate significantly decreased in the *OE-BnCKX5* lines compared with the WT plants under the mannitol treatments (Supplementary Figures 10, 11). These results suggest the *BnCKX5* overexpression increases the sensitivity to salt and mannitol stresses at the germination stage. However, the detailed molecular mechanism mediating the adverse effects of salt and mannitol stresses at the germination stage through *BnCKX5* remains to be further investigated.

### ***BnERF3* Overexpression Increased the Sensitivity to Salt and Mannitol Stresses at the Germination Stage**

By analyzing SNPs sequence variations of genes, we totally identified 38 genes by SNPs cluster on ChrA06 within 200 kb upstream and downstream of the candidate SNPs, from BnvaA0601466004 to BnvaA0601655665 of SPAD\_R2 and BnvaA0601570302 of RL\_R1 (Figures 4A,B and Supplementary Table 14). Moreover, among these genes, BnaA06g02670D, whose expression was found to be significantly induced by salt stress and dehydration treatment, has not yet been reported to be related to salt stress in *B. napus*. Thus, we focused on the BnaA06g02670D for further study (Figure 4C, Supplementary Figure 6, and Supplementary Tables 15, 17) (see text footnote 1) (Zhang et al., 2019). BnaA06g02670D named *BnERF3* is a homolog of *Arabidopsis* ERF3 belonging to the AP2/ERF subfamily, which encodes an ethylene response transcription factor and plays a very important role in signal transduction of many adversity stresses. However, whether ERF3 plays a role in plant salt tolerance remains unknown (Zhang and Huang, 2010). *BnERF3* consists of one exon with pairwise LD correlations, which presents rich SNP sequence variations leading to amino acids changes ( $r^2 > 0.5$ ) (Figure 4D and Supplementary Table 20). The haplotypes of *BnERF3* were grouped into 4 haplotypes including hap.A, hap.B, hap.C, and hap.D type accessions (Supplementary Table 21). The absolute and relative value of root length (RL) in the Hap.D type accessions were significantly less than that in hap.A, hap.B, and hap.C under salt stress (Figures 4E–G and Supplementary Table 21). However, the absolute and relative values of chlorophyll content (SPAD) in the hap.D type accessions were significantly higher than that in hap.A, hap.B and hap.C type accessions under normal and salt stress conditions (Figures 4H–J and Supplementary Table 21). Therefore, *BnERF3* was considered as a candidate gene for salt stress response and showed a rich SNPs variation among 505 *B. napus* accessions. The identified extreme haplotypes related to salt tolerance would be useful for breeding salt-tolerant *B. napus* in the future.

To examine whether *BnERF3* participates in response to salt stress, seeds of *BnERF3*-overexpressing (*OE-BnERF3*) plants and WT were sowed under the 0, 50, 100, 125, 150, 175, 200, and 225 mmol NaCl for 9 days (Figure 4K and Supplementary Figures 12, 13). Germination rates significantly decreased for the *OE-BnERF3* lines compared with the WT plants under the salt

<sup>2</sup><https://bigd.big.ac.cn/>

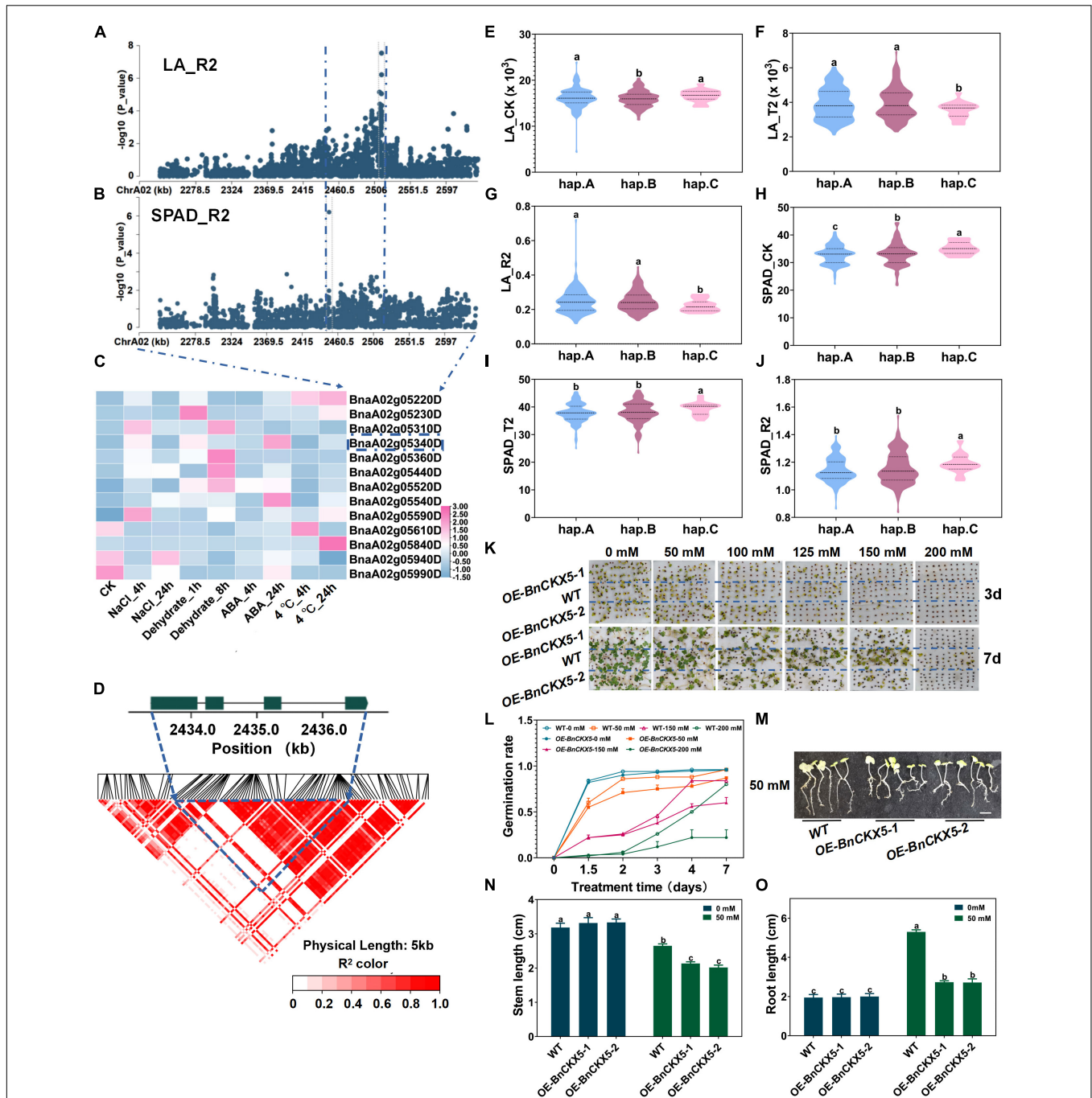


**FIGURE 3 |** Gene location and function research of *BnCKX5* under salt stress. **(A)** Zoom-in of the Manhattan plot on ChrA02 with co-localized locus. These points represented the log-transformed *P*-values for variants from GWAS of root length (RL\_R1) at the germination stage. **(B)** Zoom-in of the Manhattan plot on ChrA02 with co-localized locus. These points represented the log-transformed *P*-values for variants from GWAS of chlorophyll content (SPAD\_R2) at the seedling stage. **(C)** Gene expression of candidate genes identified within 200kb upstream or downstream of the associated SNPs under 200 mM NaCl, 25 μM ABA or 4°C low-temperature stress for 4 and 24h and dehydration condition for 1h and 8h in *B. napus* cultivar Zhong Shuang 11 ('ZS11'). **(D)** LD heatmap within 1kb upstream or downstream of *BnCKX5*. **(E–G)** Boxplots of haplotypes for the absolute and relative value of the root length (RL) at germination stage (RL\_CK, **E**; RL\_T1, **F**; and RL\_R1, **G**). Values were means ± SD and different letters indicate differences at  $P \leq 0.05$  using two-way ANOVA. **(H–J)** Boxplots of haplotypes for the absolute and relative value of different stress conditions and control with the chlorophyll content (SPAD) at seedling stage (SPAD\_CK, **H**; SPAD\_T2, **I**; and SPAD\_R2, **J**). Values were means ± SD ( $n = 6$  replicates) and different letters indicate differences at  $P \leq 0.05$  using two-way ANOVA. **(K,L)** Comparison of the germination rate (FYL, **K,L**) of wild type (Westar) and *BnCKX5* overexpression (*OE-BnCKX5*) under control and salt (0, 50, 100, 125, 150, 175, 200, 225, and 250 mM NaCl) conditions. Values were means ± SD ( $n = 2$  replicates). **(M–O)** Comparison of the shoot length (SL, **N**) and root length (RL, **O**) of wild type (Westar) and *BnCKX5* overexpression (*OE-BnCKX5*) under control and salt (0, 50, 100, 125, 150, 175, 200, 225, and 250 mM NaCl, **M**) conditions. Scale bar = 1.5 cm. Values were means ± SD ( $n = 6$  replicates) and different letters indicate differences at  $P \leq 0.05$  using two-way ANOVA.

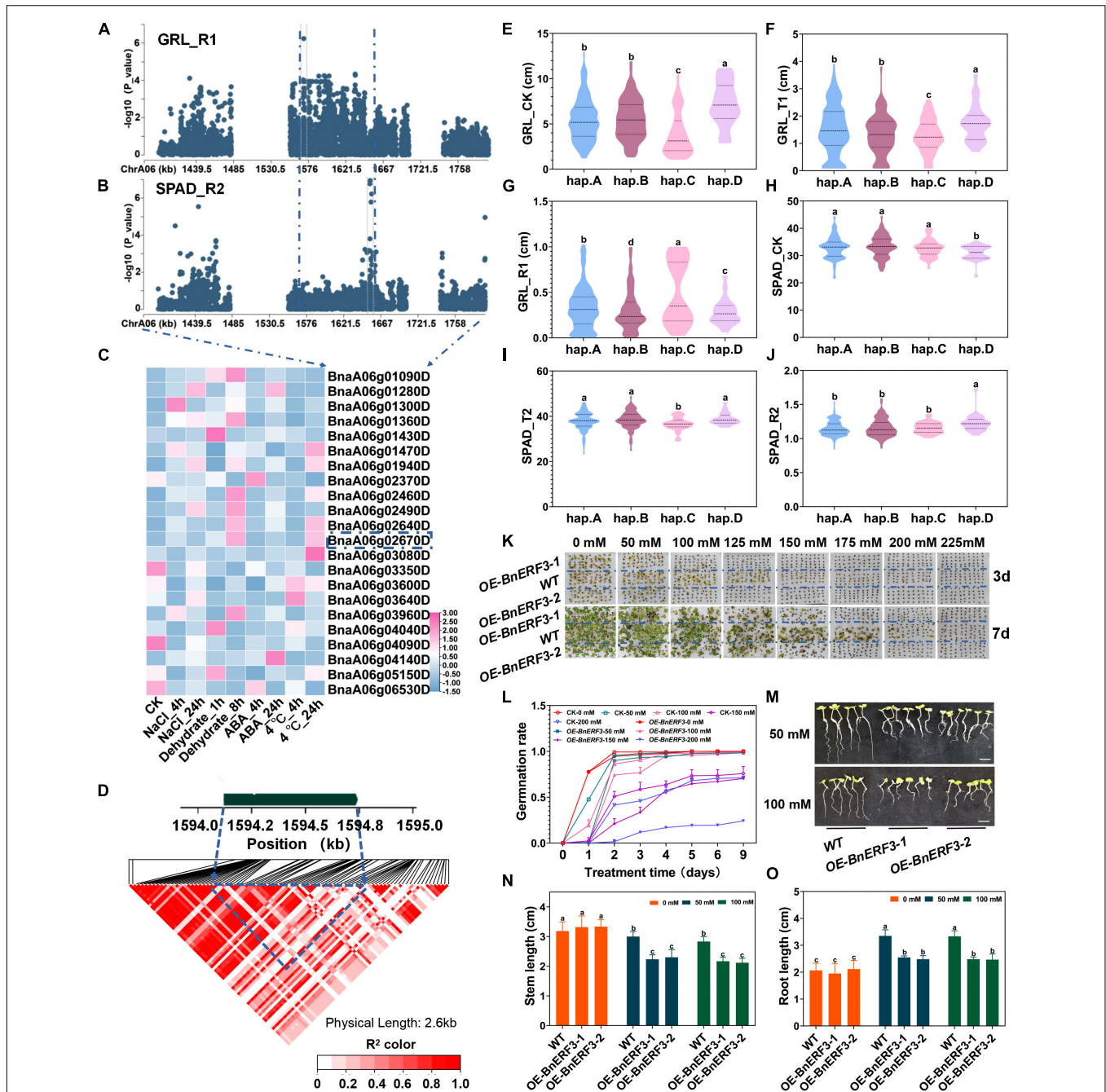


**FIGURE 4 |** Gene location and function research of *BnERF3* under salt stress. **(A)** Zoom-in of the Manhattan plot on ChrA06 with co-localized locus. These points represented the log-transformed *P*-values for variants from GWAS of root length (RL\_R1) at the germination stage. **(B)** Zoom-in of the Manhattan plot on ChrA06 with co-localized locus. These points represented the log-transformed *P*-values for variants from GWAS of chlorophyll content (SPAD\_R2) at the seedling stage. **(C)** Gene expression of candidate genes identified within 200kb upstream or downstream of the associated SNPs under 200 mM NaCl, 25 μM ABA or 4°C low-temperature stress for 4 and 24h and dehydration condition for 1 and 8h in *B. napus* cultivar Zhong Shuang 11 ("ZS11"). **(D)** LD heatmap within 1kb upstream or downstream of *BnERF3*. **(E–G)** Boxplots of haplotypes for the absolute and relative value of different stress conditions and control with the root length (RL) at germination stage (RL\_CK, **E**; RL\_T1, **F**; RL\_R1, **G**). Values were means ± SD and different letters indicate differences at *P* ≤ 0.05 using two-way ANOVA. **(H–J)** Boxplots of haplotypes for the absolute and relative value of different stress conditions and control with the chlorophyll content (SPAD) at seedling stage (SPAD\_CK, **H**; SPAD\_T2, **I**; SPAD\_R2, **J**). Values were means ± SD (*n* = 6 replicates) and different letters indicate differences at *P* ≤ 0.05 using two-way ANOVA. **(K,L)** Comparison of the germination rate (FYL, **K,L**) of wild type (Westar) and *BnERF3* overexpression (OE-*BnERF3*) under control and salt (0, 50, 100, 125, 150, 175, 200, 225, and 250 mM NaCl) conditions. Values were means ± SD (*n* = 2 replicates) and different letters indicate differences at *P* ≤ 0.05 using two-way ANOVA. **(M–O)** Comparison of the shoot length (SL, **N**) and root length (RL, **O**) of wild type (Westar) and *BnERF3* overexpression (OE-*BnERF3*) under control and salt (0, 50, 100, 125, 150, 175, 200, 225, and 250 mM NaCl, **M**) conditions. Values were means ± SD (*n* = 2 replicates). Scale bar = 1.5 cm. Values were means ± SD (*n* = 6 replicates) and different letters indicate differences at *P* ≤ 0.05 using two-way ANOVA.

treatment (Figure 4L). The stem length and root length of *OE-BnERF3* were significantly lower than that of WT under 50 mmol NaCl (Figures 4M–O). In addition, seeds of *OE-BnERF3* lines and WT have sowed under 0, 50, 100, 125, 150, 175, 200, and 225 mmol mannitol for 9 days. Germination rates significantly decreased in the *OE-BnERF3* lines compared with the WT plants under the mannitol treatments (Supplementary Figures 14, 15). These results suggest the overexpression of *BnERF3* increases the sensitivity to salt and mannitol stresses at the germination stage. However, the regulation mechanism of *BnERF3* involved in response to salt and mannitol stresses at the germination stage needs further investigation.

## DISCUSSION

Seed germination has significant influences on seedling establishment and yield performance. Germination speed under different stress conditions is a key element of vigorous seeds to measure the resistance of seed germination (Finch-Savage et al., 2010; Hatzig et al., 2015). In this study, we determined the response to salt stress at seed germination and seedling stages in 505 accessions of *B. napus*. Four phenotypic indexes and 10 growth and physiological traits were obtained at seed germination (Supplementary Tables 2, 3) and seedling stages (Supplementary Tables 2, 4), respectively.

The genetic effect and treatment effect ( $G\_effect$  and  $E\_effect$ ,  $P \leq 0.05$ ) could better represent the genotype effect and treatment effect, which were significant for all traits under salt stress (Supplementary Table 10). We found that the salt stress could significantly inhibit the plant height, root length, leaf area, aboveground dry weight and total dry weight at the seedling stage, and germination rate, shoot length, and root length at germination stage compared with control. On the contrary, salt stress significantly increased the REC, MDA, and SPAD. The broad-sense heritability could better represent the genotypic effect of all traits ranging from 1.31E-06 (GSL) to 0.664 (SPAD). Smaller plants with lower STCs were observed under salt stress. A positive correlation was observed between normal and salt stress conditions. The correlation coefficients of all traits were calculated at germination and seedling stages. The ADB was significantly correlated with TDW and LA ( $p < 001$ ). The germination potential was positively correlated with germination rate, shoot length, and root length under salt stress ( $p < 0.05$ ), in accordance with the previous studies (Taghvaei et al., 2012; Amlca and Yaldz, 2017). Our findings revealed that the traits of germination were not significantly correlated with the seedling traits, suggesting that the regulatory mechanism of salt stress responses was likely to be different between the germination and seedling stages. These results were consistent with a previous study (Wan et al., 2017).

Two previous two studies have performed GWAS to explore the genetic basis of salt stress responses at the seedling stage in 85 and 368 inbred *B. napus* lines (Yong et al., 2015; Wan et al., 2017). Though many QTLs and candidate genes related to salt stress at the seedling stage were identified, no candidate gene has been functionally validated under salt stress in *B. napus*

until now. Using a GWAS approach, we mapped 31 salts stress-related QTLs by GWAS of 16 STCs to investigate the genetic basis of salt stress tolerance of *B. napus* (Supplementary Table 11). However, parts of those SNPs could be false positives to salt stress responses. In addition, the lack of overlapped QTLs can also be the consequence of the weak power to detect the many micro-effect genes, which probably underlie the salt stress responses. Detection power was reduced by the low heritability observed in our salt stress conditions at germination and seedling stages, respectively. A total of 75 co-localized and special SNPs were found by Venn analysis between the two stages (Supplementary Table 12). Therefore, we believe that our method is trustworthy.

In addition, we totally identified 177 candidate genes at the germination stage (Supplementary Table 13) and 228 candidate genes (Supplementary Table 14) at the seedling stage, which are differentially expressed under salt stress, respectively (see text footnote 1) (Zhang et al., 2019). Some candidate genes identified from the GWAS results have been reported to be related to salt stress responses, such as BnaA03g43130D (*RAB*), BnaA05g01580D (*ABI1*), BnaA07g12170D (*ABA1*), BnaA10g29660D (*SOS3*), and BnaC07g25850D (*ABI5*) (Yong et al., 2015). Moreover, we also mapped some candidate genes, which also were identified in a previous study (Huang et al., 2012). BnaA01g02240D and BnaA01g02100D were identified for the salt tolerance index of root length (ST-RL). BnaA05g03980D, BnaA05g05230D, BnaA05g04990D, BnaA07g22240D, and BnaA07g22790D were identified for shoot length (ST-SL). BnaA01g12890D was identified for shoot fresh weight (ST-SFW) (Wan et al., 2017). Therefore, we believed that it was a reliable method to identify candidate genes related to salt stress. Interestingly, some of these candidate genes have not yet been known to be involved in salt stress responses. Additionally, BnaA02g03750D (AT5G17860.1) is a calcium exchanger protein. BnaA06g01090D (AT1G53170.1) belongs to the AP2/ERF subfamily, which encodes an ethylene response factor transcription factor and plays an important role in signal transduction of many adversity stresses (Savitch et al., 2005). BnaC05g00520D (AT1G01490.2) encodes a heavy metal transport/detoxification superfamily protein, which plays a role in ion transportation. BnaA02g07120D and BnaA02g07110D (AT5G59310.1) encode lipid transfer proteins. BnaA02g05360D (AT5G21940.1) encodes a histidine kinase. These identified candidate genes were also found to be differentially expressed under salt, drought stress, or ABA treatment (see text footnote 1) (Zhang et al., 2019).

Additionally, the function of two identified candidate genes by transgenic verification, which are *BnCKX5* and *BnERF3*, has also not yet been reported to be related to salt stress. BnaA02g05340D (*BnCKX5*) encoding a cytokinin dehydrogenase is involved in the cytokinin metabolic process. Previous studies have discovered that the *ckx3 ckx5* double mutants in *Arabidopsis thaliana* form large inflorescences, floral meristems, and more ovules, thereby increasing the number of kernels per silique (Liu et al., 2018). Four *BnCKX3* and two *BnCKX5* genes were to be regulators of reproductive development in the allotetraploid *B. napus*. *ckx3 ckx5* mutants increased cytokinin concentration

and larger and more active inflorescence meristems (Ireen et al., 2020). *PsCKX2* and *PsCKX5* formed citrus dwarf rootstock with a stronger root system with more lateral roots in *Poncirus trifoliata* (Ma et al., 2016). *BnaA06g02670D* (*BnERF3*) encodes a member of the ethylene response factor subfamily and is an AP2 transcription factor, which negatively regulates the ethylene-activated signaling pathway. *AtERF4* encoding an AP2 transcriptional repressor modulate ethylene and abscisic acid responses in *Arabidopsis* (Zhen et al., 2005). Therefore, we are curious about whether *BnCKX5* and *BnERF3* have functions in the adaptation of *B. napus* to salt stress. Our results revealed that *BnCKX5* and *BnERF3* played positive roles in response to salt and mannitol stresses in *B. napus*. However, more studies are needed to unveil the molecular mechanism of *BnCKX5* and *BnERF3* regulation in response to salt stress. These results suggest that GWAS is employed not only to confirm the presence of allelic differences in known salt tolerance-related genes but also to identify QTLs of which the causal gene is not annotated yet to be involved in salt tolerance. Our study provided an efficient way to reveal the complex genetic architecture of salt stress tolerance to *B. napus*.

## CONCLUSION

Our results revealed significant natural variation for many phenotypic indexes under salt stress at the germination and seedling stages and rich genetic variation of candidate genes related to salt stress responses. Many traits were correlated to salt stress response, indicating the overlap in salt regulatory networks or correlated responses of these traits to selection. Many candidate genes with unknown function in salt stress responses, such as *BnCKX5* and *BnERF3*, were identified based on differential expression under salt stress by haplotype analyses and genetic transformation. *BnCKX5* and *BnERF3* overexpression were found to increase the sensitivity to salt and mannitol stresses at the germination stage. Additionally, some salt-tolerant and salt-sensitive accessions have been identified as breeding materials for the genetic improvement of salt stress tolerance

## REFERENCES

- Amlca, M., and Yaldz, G. (2017). Effect of salt stress on seed germination, shoot and root length in *Basil* (*Ocimum basilicum*). *ISME* 4, 69–76. doi: 10.21448/ijsm.356250
- Apse, M. P., Aharon, G. S., Snedden, W. A., and Blumwald, E. (1999). Salt tolerance conferred by overexpression of a vacuolar  $\text{Na}^+/\text{H}^+$  antiporter in *Arabidopsis*. *Science* 285, 1256–1258. doi: 10.1126/science.285.5431.1256
- Awlia, M., Nigro, A., Fajkus, J., Schmoedel, S. M., Negro, S., Santelia, D., et al. (2016). High-throughput non-destructive phenotyping of traits that contribute to salinity tolerance in *Arabidopsis thaliana*. *Front. Plant Sci.* 7:1414. doi: 10.3389/fpls.2016.01414
- Barragan Borrero, V., Leidi, E., Andrés, Z., Rubio, L., Luca, A., Fernández, J., et al. (2012). Ion exchangers *NHX1* and *NHX2* mediate active potassium uptake into vacuoles to regulate cell turgor and stomatal function in *Arabidopsis*. *Plant Cell* 24, 1127–1142. doi: 10.1105/tpc.111.095273
- Bates, L. S., Waldren, R. P., and Teare, I. D. (1973). Rapid determination of free proline for water-stress studies. *Plant Soil* 39, 205–207. doi: 10.1007/BF00018060

of *B. napus*. This study provided insights into the genetic architecture of salt tolerance at germination and seedling stages by GWAS and would be useful for genetic improvement of salt tolerance by breeding in *B. napus*.

## DATA AVAILABILITY STATEMENT

The original contributions presented in the study are included in the article/**Supplementary Material**, further inquiries can be directed to the corresponding author.

## AUTHOR CONTRIBUTIONS

XY and LG designed the research. GZ, JZ, YP, ZT, LL, LY, CJ, SE, XY, and SL performed the experiments or analyzed the data. GZ, LG, and XY analyzed the data and wrote the manuscript. All authors contributed to the article and approved the submitted version.

## FUNDING

This study was supported by the National Key Research and Development Plan of China (2016YFD0101000).

## ACKNOWLEDGMENTS

We appreciate the instructive suggestions from LY and SL and the technical support from Di Wu.

## SUPPLEMENTARY MATERIAL

The Supplementary Material for this article can be found online at: <https://www.frontiersin.org/articles/10.3389/fpls.2021.772708/full#supplementary-material>

- Bedard, K., and Krause, K. H. (2007). The *NOX* family of ROS-generating *NADPH* oxidases: physiology and pathophysiology. *Physiol. Rev.* 87, 245–313. doi: 10.1152/physrev.00044.2005
- Brini, F., Hanin, M., Mezghani, I., Berkowitz, G. A., and Masmoudi, K. (2007). Overexpression of wheat  $\text{Na}^+/\text{H}^+$  antiporter *TNXX1* and  $\text{H}^+$ -pyrophosphatase *TVPI* improve salt- and drought-stress tolerance in *Arabidopsis thaliana* plants. *J. Exp. Bot.* 58, 301–308. doi: 10.1093/jxb/erl251
- Campbell, M. T., Knecht, A. C., Berger, B., Brien, C. J., Wang, D., and Walia, H. (2015). Integrating image-based phenomics and association analysis to dissect the genetic architecture of temporal salinity responses in rice. *Plant Physiol.* 168:1476. doi: 10.1104/pp.15.00450
- Chen, D., Neumann, K., Friedel, S., Kilian, B., Chen, M., Altmann, T., et al. (2014). Dissecting the phenotypic components of crop plant growth and drought responses based on high-throughput image analysis. *Plant Cell* 26:4636. doi: 10.1105/tpc.114.129601
- Dai, C., Li, Y., Li, L., Du, Z., and Lu, S. (2020). An efficient agrobacterium-mediated transformation method using hypocotyl as explants for *Brassica napus*. *Mol. Breed.* 40:96. doi: 10.1007/s11032-020-01174-0

- De, R., Bush, W. S., and Moore, J. H. (2014). Bioinformatics challenges in genome-wide association studies (GWAS). *Methods Mol. Biol.* 1168, 63–81. doi: 10.1007/978-1-4939-0847-9\_5
- Fan, Y., Zhou, G., Shabala, S., Chen, Z. H., Cai, S., Li, C., et al. (2016). QTL mapping barley evaluation methods genome wide association study salinity tolerance. *Front. Plant Sci.* 7:946. doi: 10.3389/fpls.2016.00946
- Finch-Savage, W. E., Clay, H. A., Lynn, J. R., and Morris, K. (2010). Towards a genetic understanding of seed vigour in small-seeded crops using natural variation in *Brassica oleracea*. *Plant Sci.* 179, 582–589. doi: 10.1016/j.plantsci.2010.06.005
- Gomes-Filho, E., Lima, C. R. F. M., Costa, J. H., da Silva, A. C. M., da Guia Silva Lima, M., de Lacerda, C. F., et al. (2008). Cowpea ribonuclease: properties and effect of NaCl-salinity on its activation during seed germination and seedling establishment. *Plant Cell* 27, 147–157. doi: 10.1007/s00299-007-0433-5
- Guo, Z., Yang, W., Chang, Y., Ma, X., Tu, H., Xiong, F., et al. (2018). Genome-wide association studies of image traits reveal the genetic architecture of drought resistance in rice. *Mol. Plant* 11, 789–805. doi: 10.1016/j.molp.2018.03.018
- Hatzig, S. V., Frisch, M., Breuer, F., Nesi, N., and Snowdon, R. J. (2015). Genome-wide association mapping unravels the genetic control of seed germination and vigor in *Brassica napus*. *Front. Plant Sci.* 6:221. doi: 10.3389/fpls.2015.00221
- Hickey, L. T. A. N. H., Robinson, H., Jackson, S. A., Leal-Bertioli, S. C. M., Tester, M., and Wulff, B. B. H. (2019). Breeding crops to feed 10 billion. *Nat. Biotechnol.* 37, 744–754. doi: 10.1038/s41587-019-0152-9
- Hong, B. S., Zong, S. L., Ming, A. S., and Sun, Q. (2005). Dynamic changes of anti-oxidative enzymes of 10 wheat genotypes at soil water deficits. *Colloid Surf. B* 42, 187–195. doi: 10.1016/j.colsurfb.2005.02.007
- Hou, L. T., Wang, T. Y., Jian, H. J., Wang, J., Li, J. N., and Liu, L. Z. (2017). QTL Mapping for seedling dry weight and fresh weight under salt stress and candidate genes analysis in *Brassica napus* L. *Zuo Wu Xue Bao* 43:179. doi: 10.3724/sp.j.1006.2017.00179
- Huang, X., Zhao, Y., Wei, X., Li, C., Wang, A., Qiang, Z., et al. (2012). Genome-wide association study of flowering time and grain yield traits in a worldwide collection of rice germplasm. *Nat. Genet.* 44:32. doi: 10.1038/ng.1018
- Ireen, S., Marie-Therese, S., Elisabeth, O., Isabel, B., Ralf-Christian, S., and Thomas, S. (2020). Cytokinin regulates the activity of the inflorescence meristem and components of seed yield in oilseed rape. *J. Exp. Bot.* 71, 7146–7159. doi: 10.1093/jxb/era419
- Julkowska, M. M., and Testerink, C. (2015). Tuning plant signaling and growth to survive salt. *Trends Plant Sci.* 20, 586–594. doi: 10.1016/j.tplants.2015.06.008
- Kang, Y., Torres-Jerez, I., An, Z., Greve, V., Huhman, D., Krom, N., et al. (2019). Genome-wide association analysis of salinity responsive traits in *Medicago truncatula*. *Plant Cell Environ.* 42, 1513–1531. doi: 10.1111/pce.13508
- Khan, F., and Hakeem, K. R. (2013). "Cell signaling during drought and salt stress," in *Plant Signaling-Understanding the Molecular Cross-talk*, eds K. R. Hakeem, R. Rehman, and I. Tahir (Berlin: Springer-verlag), 227–239. doi: 10.1007/978-81-322-1542-4\_11
- Khan, M. A., and Weber, D. J. (2006). *Ecophysiology Of High Salinity Tolerant Plants*. Berlin: Springer. doi: 10.1007/1-4020-4018-0
- Khedr, A., Abbas, M. A., Wahid, A., Quick, W. P., and Abogadallah, G. M. (2015). Proline induces the expression of salt-stress-responsive proteins and may improve the adaptation of *Pantratum maritimum* L. to salt-stress. *J. Exp. Bot.* 54, 2553–2562. doi: 10.1093/jxb/erg277
- Lang, L., Xu, A., Ding, J., Zhang, Y., Zhao, N., Tian, Z., et al. (2017). Quantitative trait locus mapping of salt tolerance and identification of salt-tolerant genes in *Brassica napus* L. *Front. Plant Sci.* 8:1000. doi: 10.3389/fpls.2017.01000
- Li, H., and Durbin, R. (2009). Fast and accurate short read alignment with *Burrows-wheeler* transform. *Bioinformatics* 25, 1754–1760. doi: 10.1093/bioinformatics/btp324
- Lin, H. X., Zhu, M. Z., Yano, M., Gao, J. P., Liang, Z. W., Su, W. A., et al. (2004). QTLs for Na<sup>+</sup> and K<sup>+</sup> uptake of the shoots and roots controlling rice salt tolerance. *Theor. Appl Genet.* 108, 253–260. doi: 10.1007/s00122-003-1421-y
- Listgarten, J., Lippert, C., and Heckerman, D. (2013). FaST-LMM-select for addressing confounding from spatial structure and rare variants. *Nat. Genet.* 45, 470–471. doi: 10.1038/ng.2620
- Liu, P., Zhang, C., Ma, J. Q., Zhang, L. Y., Yang, B., Tang, X. Y., et al. (2018). Genome-wide identification and expression profiling of cytokinin oxidase/dehydrogenase (CKX) genes reveal likely roles in pod development and stress responses in oilseed rape (*Brassica napus* L.). *Genes* 9:168. doi: 10.3390/genes9030168
- Long, W., Zou, X., and Zhang, X. (2015). Transcriptome analysis of canola (*Brassica napus*) under salt stress at the germination stage. *PLoS One* 10:e0116217. doi: 10.1371/journal.pone.0116217
- Ly, Y., Guo, Z., Li, X., Ye, H., Li, X., and Xiong, L. (2016). New insights into the genetic basis of natural chilling and cold shock tolerance in rice by genome-wide association analysis. *Plant Cell Environ.* 39, 556–570. doi: 10.1111/pce.12635
- Ma, L., Ye, J., Yang, Y., Lin, H., Yue, L., Luo, J., et al. (2019). The SOS2-SCaBP8 complex generates and fine-tunes an *AtANN4*-dependent calcium signature under salt stress. *Dev. Cell* 48:e695. doi: 10.1016/j.devcel.2019.02.010
- Ma, Y. Y., Li, Z., Xie, R., He, S. L., and Deng, L. (2016). Genome-wide identification and analysis of CKX genes in *Poncirus trifoliata*. *Hortic. Sci. Biotech.* 91, 1–11. doi: 10.1080/14620316.2016.1194171
- Mba, C., Afza, R., Jain, S. M., Gregorio, G. B., and Zapata-Arias, F. J. (2007). *Induced Mutations For Enhancing Salinity Tolerance In Rice*. Berlin: Springer, 413–454. doi: 10.1007/978-1-4020-5578-2\_17
- Monirifar, H., and Barghi, M. (2009). Identification and selection for salt tolerance in *Alfalfa (Medicago sativa* L.) ecotypes via physiological traits. *Not. Sci. Biol.* 1:63. doi: 10.15835/nsb113498
- Morton, M. J. L., Awlia, M., Al-Tamimi, N., Saade, S., Pailles, Y., Negrao, S., et al. (2019). Salt stress under the scalpel dissecting the genetics of salt tolerance. *Plant J.* 97, 148–163. doi: 10.1111/tpj.14189
- Munns, R. (2005). Genes and salt tolerance: bringing them together. *New Phytol.* 167, 645–663. doi: 10.1111/j.1469-8137.2005.01487.x
- Munns, R., and Tester, M. (2008). Mechanisms of salinity tolerance. *Annu. Rev. Plant Biol.* 59, 651–681. doi: 10.1146/annurev.arplant.59.032607.092911
- Munns, R., James, R. A., Xu, B., Athman, A., Conn, S. J., Jordans, C., et al. (2012). Wheat grain yield on saline soils is improved by an ancestral Na (+) transporter gene. *Nat. Biotechnol.* 30, 360–364. doi: 10.1038/nbt.2120
- Patishan, J., Hartley, T. N., Fonseca de Carvalho, R., and Maathuis, F. J. M. (2018). Genome-wide association studies to identify rice salt-tolerance markers. *Plant Cell Environ.* 41, 970–982. doi: 10.1111/pce.12975
- Pearson, T. A., and Manolio, T. A. (2008). How to interpret a genome-wide association study. *JAMA* 299, 1335–1344. doi: 10.1001/jama.299.11.1335
- Rehman, S., Harris, P., Bourne, W., and Wilkin, J. (2000). The relationship between Ions, vigour and salinity tolerance of *Acacia* Seeds. *Plant Soil* 220, 229–233. doi: 10.1023/A:1004701231183
- Savitch, L. V., Allard, G., Seki, M., Robert, L. S., Tinker, N. A., and Huner, N. (2005). The effect of overexpression of two like transcription factors on photosynthetic capacity and freezing tolerance in *Brassica napus*. *Plant Cell Physiol.* 46, 1525–1539. doi: 10.1093/pcp/pci165
- Shi, H., Quintero, F. J., Pardo, J. M., and Zhu, J. K. (2002). The putative plasma membrane Na<sup>+</sup>/H<sup>+</sup> antiporter *SOS1* controls long-distance Na<sup>+</sup> transport in plants. *Plant Cell* 14, 465–477. doi: 10.1105/tpc.010371.et
- Song, W., and Liu, M. (2017). Farmland conversion decreases regional and national land quality in China. *Land Degrad. Dev.* 28, 459–471. doi: 10.1002/ldr.2518
- Taghvaei, M., Khaef, N., and Sadeghi, H. (2012). The effects of salt stress and prime on germination improvement and seedling growth of *Calotropis procera* L. seeds. *JEE* 35, 73–78. doi: 10.5141/JEFB.2012.011
- Tang, S., Zhao, H., Lu, S., Yu, L., Zhang, G., Zhang, Y., et al. (2021). Genome- and transcriptome-wide association studies provide insights into the genetic basis of natural variation of seed oil content in *Brassica napus*. *Mol. Plant* 14, 470–487. doi: 10.1016/j.molp.2020.12.003
- Tyerman, S. D., and Munns, R. (2019). Energy costs of salinity tolerance in crop plants. *New Phytol.* 221, 25–29. doi: 10.1111/nph.15555
- Wan, H., Chen, L., Guo, J., Li, Q., Wen, J., Yi, B., et al. (2017). Genome-wide association study reveals the genetic architecture underlying salt tolerance-related traits in rapeseed (*Brassica napus* L.). *Front. Plant Sci.* 8:593. doi: 10.3389/fpls.2017.00593
- Wang, Y. X., Sun, G. R., Wang, J. B., Cao, W. Z., and Lu, Z. H. (2006). Relationships among MDA content, plasma membrane permeability and the chlorophyll fluorescence parameters of *Puccinellia tenuiflora* seedlings under NaCl stress. *Sheng Tai Xue Bao* 26, 122–129.
- Yang, W., Guo, Z., Huang, C., Wang, K., Jiang, N., Feng, H., et al. (2015). Genome-wide association study of rice (*Oryza sativa* L.) leaf traits with a high-throughput leaf scorer. *J. Exp. Bot.* 66, 5605–5615. doi: 10.1093/jxb/erv100

- Yong, H. Y., Wang, C., Bancroft, I., Li, F., Wu, X., Kitashiba, H., et al. (2015). Identification of a gene controlling variation in the salt tolerance of rapeseed (*Brassica napus* L.). *Planta* 242, 313–326. doi: 10.1007/s00425-015-2310-8
- Yong, H. Y., Zou, Z., Kok, E. P., Kwan, B. H., and Nishio, T. (2014). Comparative transcriptome analysis of leaves and roots in response to sudden increase in salinity in *Brassica napus* by RNA-seq. *J. Biomed. Biotechnol.* 2014:467395. doi: 10.1155/2014/467395
- Yu, J., Zao, W., He, Q., Kim, T. S., and Park, Y. J. (2017). Genome-wide association study and gene set analysis for understanding candidate genes involved in salt tolerance at the rice seedling stage. *Mol. Genet Genomics* 292, 1391–1403. doi: 10.1007/s00438-017-1354-9
- Yu, J., Zhao, W., Tong, W., He, Q., Yoon, M. Y., Li, F. P., et al. (2018). A genome-wide association study reveals candidate genes related to salt tolerance in rice (*Oryza sativa*) at the germination stage. *Int. J. Mol. Sci.* 19:3145. doi: 10.3390/ijms19103145
- Zhang, H. X., Hodson, J. N., and Williams, J. P. (2001). Engineering salt-tolerant *Brassica* plants: characterization of yield and seed oil quality in transgenic plants with increased vacuolar sodium accumulation. *Proc. Natl. Acad. Sci.* 98, 12832–12836.
- Zhang, Y., Ali, U., Zhang, G., Yu, L., Fang, S., Iqbal, S., et al. (2019). Transcriptome analysis reveals genes commonly responding to multiple abiotic stresses in rapeseed. *Mol. Breed.* 39:158 doi: 10.1007/s11032-019-1052-x
- Zhang, Z., and Huang, R. (2010). Enhanced tolerance to freezing in tobacco and tomato overexpressing transcription factor *TERF2/LeERF2* is modulated by ethylene biosynthesis. *Plant Mol. Biol.* 73, 241–249. doi: 10.1007/s11103-010-9609-4
- Zhao, B. Y., Hu, Y. F., Li, J. J., Xuan, Y., and Liu, K. D. (2016). BnaABF2, a bZIP transcription factor from rapeseed (*Brassica napus* L.), enhances drought and salt tolerance in transgenic *Arabidopsis*. *Bot. Stud.* 57:12. doi: 10.1186/s40529-016-0127-9
- Zhen, Y., Tian, L., Latoszek-Green, M., Brown, D., and Wu, K. (2005). *Arabidopsis* *ERF4* is a transcriptional repressor capable of modulating ethylene and abscisic acid responses. *Plant Mol. Biol.* 58, 585–596. doi: 10.1007/s11103-005-7294-5
- Zhu, J. K. (2001b). The salinity challenge. *New Phytol.* 225, 1047–1048. doi: 10.1111/nph.16357
- Zhu, J. K. (2001a). Cell signaling under salt, water and cold stresses. *Curr. Opin. Plant Biol.* 4, 401–406. doi: 10.1016/S1369-5266(00)00192-8
- Zhu, J. K. (2002). Salt and drought stress signal transduction in plants. *Annu. Rev. Plant Biol.* 53, 247–273. doi: 10.1146/annurev.arplant.53.091401.143329
- Zhu, J. K. (2016). Abiotic stress signaling and responses in plants. *Cell* 167, 313–324. doi: 10.1016/j.cell.2016.08.029

**Conflict of Interest:** The authors declare that the research was conducted in the absence of any commercial or financial relationships that could be construed as a potential conflict of interest.

**Publisher's Note:** All claims expressed in this article are solely those of the authors and do not necessarily represent those of their affiliated organizations, or those of the publisher, the editors and the reviewers. Any product that may be evaluated in this article, or claim that may be made by its manufacturer, is not guaranteed or endorsed by the publisher.

Copyright © 2022 Zhang, Zhou, Peng, Tan, Li, Yu, Jin, Fang, Lu, Guo and Yao. This is an open-access article distributed under the terms of the Creative Commons Attribution License (CC BY). The use, distribution or reproduction in other forums is permitted, provided the original author(s) and the copyright owner(s) are credited and that the original publication in this journal is cited, in accordance with accepted academic practice. No use, distribution or reproduction is permitted which does not comply with these terms.